Synthesis of metallic nanoparticles protected with *N*,*N*,*N*-trimethyl chitosan chloride via a relatively weak affinity

2006 Nanotechnology 17 4156

(http://iopscience.iop.org/0957-4484/17/16/027)

INSTITUTE OF PHYSICS PUBLISHING NANOTECHNOLOGY
Nanotechnology **17** (2006) 4156–4162 doi:10.1088/0957-4484/17/16/027

Synthesis of metallic nanoparticles protected with *N*,*N*,*N*-trimethyl chitosan chloride via a relatively weak affinity

Ya Ding[1], **Xing-Hua Xia**[1,3] **and Can Zhang**[2]

[1] Key Laboratory of Analytical Chemistry for Life Science, School of Chemistry and Chemical Engineering, Nanjing University, Nanjing 210093, People's Republic of China
[2] College of Pharmacy, China Pharmaceutical University, Nanjing 210009, People's Republic of China

E-mail: xhxia@nju.edu.cn

Received 29 April 2006, in final form 11 July 2006
Published 28 July 2006
Online at stacks.iop.org/Nano/17/4156

Abstract
A water-soluble cationic chitosan derivative, *N*,*N*,*N*-trimethyl chitosan chloride (TMC), was synthesized and used as a stabilizing reagent for the synthesis of highly stable Au, Ag and Pt nanoparticles in a single-phase of neutral aqueous solution. The morphology and stability of metallic nanoparticles were evaluated by transmission electron microscopy and UV–vis spectroscopy. The results showed that well-dispersed metallic nanoparticles have a spherical morphology with diameters of about 3 ± 0.5 nm. The prepared gold nanoparticles are stable in the aqueous solution (no significant changes in their morphology and size within 10 months) due to repulsion between the charged polymer shell coatings around the metallic nanoparticles. The relatively low affinity of TMC on gold nanoparticles was confirmed by using a ligand exchange experiment. The mechanism stabilizing the chitosan derivative and the neighbouring gold nanoparticles was identified by FTIR, ^{1}H NMR and ^{13}C NMR measurements.

1. Introduction

Since the Middle Ages it has been known that soluble gold has a high biocompatibility and curative power for various diseases, such as heart and venereal problems, dysentery, tumours and syphilis [1]. However, it is generally recognized that the surfaces of many metallic nanoparticles (NPs) of Au, Ag, Pt and Cu are charged [2], and this will cause nonspecific binding to biological molecules via electrostatic interactions. To avoid these nonspecific interactions between metallic nanoparticles and biomolecules, the preparation of metallic colloids with functional protection has become a challenging task. The Brust method was a breakthrough in this field, and concerns the synthesis of thiol-derivatized gold nanoparticles (AuNPs) in a two-phase liquid–liquid system [3]. Although alkanethiol protected gold nanoparticles can avoid electrostatic interactions with biomolecules, they will inevitably induce hydrophobic interactions. The insoluble nature of alkanethiol-protected nanoparticles makes them incompatible with biomolecules. The use of water-soluble stabilizers bearing mercapto groups, such as neutral polymers [4], carboxyl acid or carboxylate [5, 6] and peptide ligands [7], has since been developed. However, the complicated preparation process and the strong interactions of the AuNPs with the thiol ligands limit its further application. Therefore, a simple method for synthesizing functional protected metallic nanoparticles in aqueous solutions with capping by alternative ligands with weak interactions is challenging.

Citrate reduction [8] is a conventional method for the synthesis of AuNPs using carboxyl groups as ligands. Freshly prepared AuNPs are necessary for further application of this method and the preparation of water-soluble polymer modified AuNPs is essential. The synthesis of monodispersed Pt, Pd and Au nanoparticles using linear polymers, including various homopolymers and random copolymers, by chemical reduction methods using $NaBH_4$ has been developed [9–11].

[3] Author to whom any correspondence should be addressed.

Functional groups having a relatively low affinity for Au, such as cyano (–CN), pyrrolidine and amine (–NH_2) groups, are used as protecting agents. Chitosan (CS), a kind of naturally produced polysaccharide with extraordinary biocompatibility and biodegradation, has attracted much attention in this respect. Recently, multi-morphologic AuNPs have been synthesized using chitosan as both the reducing and stabilizing agent [12, 13]. Polyelectrolyte immobilized AuNP films have also been prepared by irradiation with UV light and x-rays [14, 15]. In these methods, the AuNPs were stabilized by the amine groups (–NH_2) in the main chain of the chitosan. However, since chitosan can only be dissolved in dilute acid, such as hydrochloric acid and acetic acid, the resulting gold nanoparticles prepared using these methods have limitations in biological applications. In order to achieve an efficient method for preparing AuNPs in neutral aqueous solution, the design and development of novel water-soluble polysaccharide derivatives with functional groups is needed.

Schiffrin and his co-workers have previously reported a method involving a two-phase system for the preparation of gold clusters using a quaternary ammonium bromide salt ($R_4N^+Br^-$) as the phase-transfer reagent [16]. It has been assumed that the phase-transfer reagent is specifically adsorbed on the clusters through the formation of surface ion pairs, e.g. a Br^- ion specifically attached to the Au surface. Thus, introduction of the quaternary ammonium halide salt into the chitosan structure will result in a water-soluble polysaccharide derivative for stabilizing gold nanoparticles. *N*,*N*,*N*-trimethyl chitosan chloride (TMC) is a cationic polysaccharide having the ability to form polyelectrolyte complexes with DNA or/and proteins [17–20]. It has been proved that TMC polymers with high degrees of substitution (around 40%) might be an effective and safe absorption enhancer for drug delivery [21, 22].

In this paper, a simple method for the preparation of gold nanoparticles in aqueous solution was developed. TMC was prepared and subsequently used as a capping agent for metallic nanoparticles. The morphology and stability of the nanoparticles were evaluated by transmission electron microscopy (TEM) and UV–vis spectroscopy. The shell/core structure of the polymer nanoparticles can be easily freeze-dried and stored as a powder that can subsequently be redissolved in water to yield stable aqueous dispersions for further application. The relatively low affinity of TMC towards gold nanoparticles was proved by a ligand exchange experiment using mercaptoacetic acid as a probe. The possible ligand mechanism of the nanoparticles with the capping agent was investigated by using FTIR, ^{1}H nuclear magnetic resonance (NMR) and ^{13}C NMR spectra.

2. Experimental details

2.1. Materials and methods

The synthesis of TMC and the preparation of TMC-coated gold nanoparticles can be summarized by equations (1) and (2) respectively, where BH_4^- ions act as the source of the electrons:

$$(C_6H_{10}O_4 - NH_2)_n + 3nCH_3I + NaCl \rightarrow [C_6H_{10}O_4N^+(CH_3)_3{\cdot}Cl^-]_n + NaI \quad (1)$$

$$m AuCl_4^- + [C_6H_{10}O_4N^+(CH_3)_3{\cdot}Cl^-]_n + 3m\ e^- \rightarrow (Au_m)[C_6H_{10}O_4N^+(CH_3)_3{\cdot}Cl^-]_n. \quad (2)$$

2.2. Synthesis of gold, silver and platinum nanoparticles using TMC as the stabilizer

TMC was prepared in a two-step reaction method according to Sieval *et al* [23]. The preparation of TMC-protected metallic nanoparticles was carried out in a single-phase system of sub-boiling water filtered through microporous membranes with an aperture of 0.22 μm. All glassware used was cleaned in a bath of freshly prepared aqua regia solution (HCl:HNO_3 3:1) and then rinsed thoroughly with deionized water prior to use. An aqueous solution of $HAuCl_4$ (206 μl, 60 mM) was mixed with a diluted solution of TMC (40 ml, concentration varied from 0.62 to 3.1 mM, $AuCl_4^-$:saccharide unit ratios were 1:2, 1:4, 1:8, 1:10) with vigorous stirring in an ice-water bath for 30 min. Then freshly prepared and cooled $NaBH_4$ aqueous solution (1.2 ml, 0.1 M) was added into the reaction solution, and the solution immediately turned orange. After stirring the solution for 2 h, a pink gold colloidal dispersion was obtained. TMC-protected Ag and Pt nanoparticles were synthesized in the same way. Finally, the obtained TMC-modified metal colloids were dialysed against deionized water to remove small molecules.

2.3. Synthesis of gold nanoparticles using citrate as the stabilizer

An aqueous solution of $HAuCl_4$ (206 μl, 60 mM) was added to a diluted solution of trisodium citrate (39.8 ml, 0.25 mM) with vigorous stirring in an ice-water bath for 30 min. Then a freshly prepared and cooled $NaBH_4$ aqueous solution (1.2 ml, 0.1 M) was added to the reaction system. The solution immediately turned pink. After the reaction, the solution was stirred for 2 h and a wine-red colour was obtained.

2.4. Characterization

The chemical structures of chitosan, TMC and TMC-protected gold nanoparticles in KBr discs were measured by a Tensor-27 Fourier IR spectrometer (Bruker, USA) equipped with a liquid nitrogen cooled mercury–cadmium–telluride (MCT) detector. Morphologies of all samples were characterized by a JEM-200CX TEM (JEOL, Japan) at an acceleration voltage of 200 kV. ^{1}H NMR and ^{13}C NMR spectra were performed on a Bruker (AVACE) AV-500 spectrometer. UV–vis spectra were collected on a UV-2401 PC UV–vis spectrophotometer (Shimadzu, USA).

3. Results and discussion

3.1. Nanoparticle synthesis and characterization

The preparation process of TMC and the formation of TMC-protected metallic nanoparticles are illustrated in figure 1. The chemical structure of TMC was characterized by FTIR, ^{1}H NMR and ^{13}C NMR spectra, the results are in good agreement with reference [23]. TMC is used as the stabilizer coating around the metallic nanoparticles. To compare the morphology and size distribution of the nanoparticles, freshly prepared citrate-stabilized AuNPs and TMC-coated gold, silver and platinum nanoparticles were characterized by TEM.

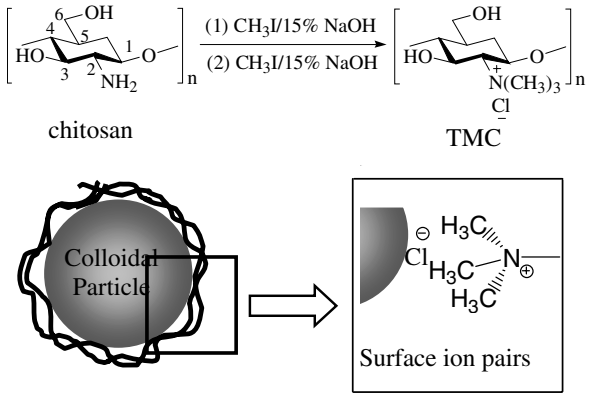

Figure 1. Schematic representation of the synthesis procedure for TMC and the formation of TMC-stabilized metallic nanoparticles.

TEM images of nanoparticles are shown in figure 2 and the mean diameters were calculated by counting 100 particles from the TEM photographs. Obviously, citrate-AuNPs have a relatively broad size distribution ranging from 5 to 8 nm (figure 2(a)), and the particles are not dispersed well due to connection by the stabilizing reagents. The TEM photograph of the freshly prepared TMC-coated AuNPs (figure 2(b)) shows that they have an average diameter of 2.9 nm with a maximum particle size distribution at 0.5–1.0 nm (figure 2(c)). After storage in the daylight at room temperature for 2 months, most of the particle diameters are unchanged but some of the gold nanoparticles grew to about 5 nm (figure 2(d)). The average diameter of the sample increased to 3.0 nm, and the size distribution became wider (figure 2(e)). Gold nanoparticles larger than five times the initial average size as reported in [24] using other block copolymers [24] were not observed in the present approach. Even with a storage time of 3 months under the same conditions, the TMC-coated gold nanoparticles were still quite stable (figure 2(f)). From the magnified TEM image presented in figure 2(g), it is clear that some external TMC polymers were coated around the gold nanoparticles, some gold particles were attached with or conjugated to polymer, and some particles consisting of just polymer also exist due to the excess TMC in the solution. It is assumed that the variety of types of polymer–particle hybrids

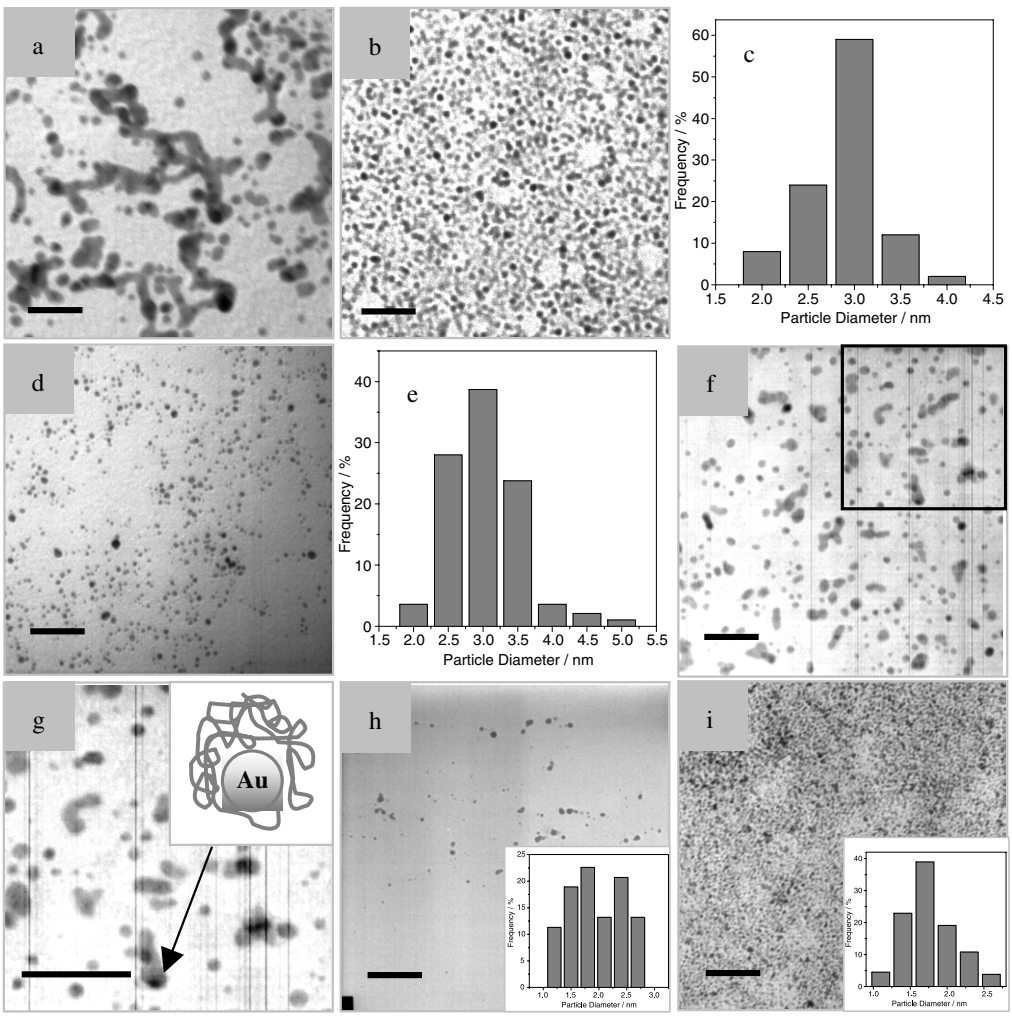

Figure 2. TEM pictures of (a) gold nanoparticles using trisodium citrate as the stabilizing reagent; (b) freshly prepared TMC-coated gold nanoparticles and (c) a histogram of their size distribution; (d) TMC-coated gold nanoparticles after storage for 2 months and corresponding histogram of their size distribution (e); (f) TMC-coated gold nanoparticles after storage for 3 months and (g) a magnified image of the black pane in image (f); (g) TMC-AgNPs and (h) TMC-PtNPs with insets of the histograms of silver and platinum size distributions. Scale bars are 25 nm.

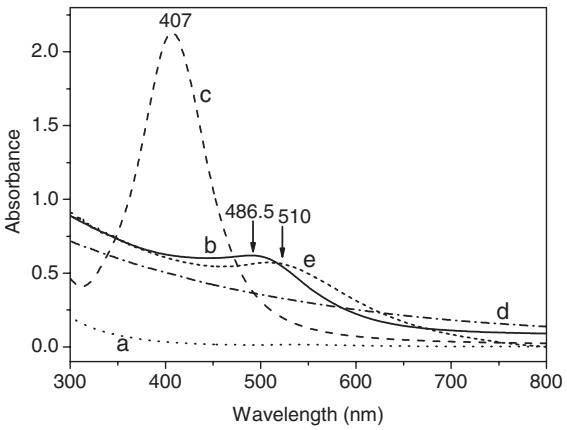

Figure 3. UV–vis absorption spectra of (a) TMC (dotted curve), (b) TMC-coated AuNPs (solid curve), (c) AgNPs (dashed curve), (d) PtNPs (dash–dotted curve) and (e) citrate-stabilized AuNPs (small dashed curve).

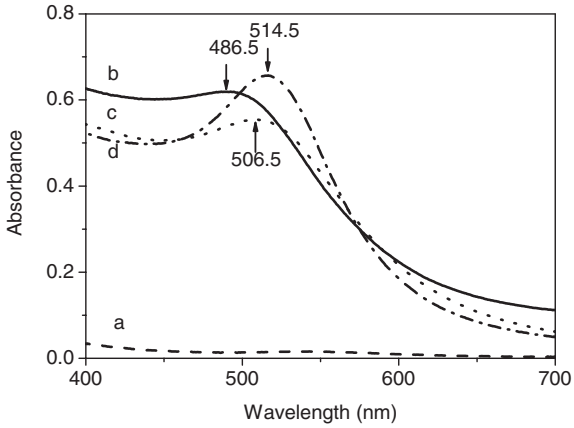

Figure 4. UV–vis absorption spectra of (a) TMC (dashed curve), (b) freshly prepared TMC-coated AuNPs (solid curve) and TMC-AuNPs stored for (c) 2 months (dotted curve) and (d) 3 months (dash–dotted curve), respectively.

can be explained by the dynamic coating and un-coating of TMC polymer around the surface of the metallic particles due to the weak affinity between TMC and gold nanoparticles. The illustration in the inset of figure 2(g) shows a typical a metallic core/polymer shell structure, indicating that the external TMC structure is associated with the surfaces of the nanoparticles. We believe that the polymer shell of the gold nanostructures, having the same charges, prevents the aggregation of metallic nanoparticles and gives TMC-AuNPs their stability in the aqueous solution. Interestingly, the polymer–nanoparticle shell/core structure can be easily freeze-dried and stored as a powder. This powder can be subsequently redissolved to yield stable aqueous dispersions. Various experiments have shown that the ratio of the metal salts to the TMC did not have any obvious effect on the morphology and size of the metallic nanoparticles. Using the same method, a transparent bright yellow silver colloid and light grey platinum colloid modified by TMC were also prepared, which also have a narrow size distribution in the nanoscale (figures 2(h) and (i)).

The optical properties of the synthesized nanoparticles were characterized using UV–vis spectroscopy (figure 3). The citrate-stabilized AuNPs display a characteristic UV–vis absorption spectrum with a plasmon band at 510 nm (figure 3, curve (e)) reflecting the existence of AuNPs of about 5–6 nm. TMC-derivatized AuNPs have a UV–vis absorption at about 486.5 nm (figure 3, curve (b)), which implies that the size of the AuNPs is less than 3 nm. In the case of silver and platinum, the UV–vis absorption spectrum of TMC-AgNPs demonstrates a sharp absorption at about 406 nm (figure 3, curve (c)), while the TMC-PtNPs do not show any special absorption (figure 3, curve (d)). The stability of TMC-coated metallic nanoparticles can be proved by UV–vis results. UV–vis absorption peaks of the TMC-AuNPs shifted to blue by 20 nm and 28 nm after 2 and 3 months, respectively (figure 4). This shift is much smaller than the reported band shift of ∼10 nm for the star-block copolymer-stabilized AuNPs 24 h after reduction [24]. It reflects the slow growth of the AuNPs under the storage conditions. The sharpening plasmon band for the stored AuNPs demonstrates that the AuNPs become gradually more uniform depending on the length of time.

From the results of TEM and UV–vis spectroscopy it can be concluded that this simple method of preparation is efficient in preparing well-dispersed gold nanoparticles with narrow distribution and stability. The present synthesis method can be easily extended to the preparation of other metallic nanoparticles which are currently under investigation. The relatively low affinity between TMC and gold nanoparticles, which is of great significance for the further application of gold nanoparticles, was investigated by a ligand-exchange experiment, as further discussed below.

3.2. Ligand mechanism discussion

Recently, Schiffrin and his co-workers reported the synthesis of gold nanoparticles with quaternary ammonium bromide salts ($R_4N^+Br^-$) as the phase-transfer reagent [16]. They proposed 'surface ion pairs' to explain the ligand mechanism in which the Br^- ion specifically adsorbs on the surfaces of the gold clusters through electrostatic interactions. However, the hypothesis of the 'surface ion pairs' mechanism has not yet been confirmed. For further discussion of the TMC-ligand mechanism in this work, FTIR, ^{1}H NMR and ^{13}C NMR spectra were obtained to compare the structure changes of TMC before and after coating around the gold nanoparticles. FTIR spectra of CS, TMC and TMC-coated gold nanoparticles are shown in figure 5. Curve (a) shows the characteristic IR features of pure CS. The absorption bands located at 1380 and 1662 cm^{-1} are due to the adsorption of amide III and amide I groups, respectively, and the band at 1598 cm^{-1} arises from the bending vibration of $–NH_2$. The absorption band at 1156 cm^{-1} can be assigned to the asymmetric stretching of the C–O–C bridge. The bands at 1075 and 1033 cm^{-1}, characteristic of the saccharine structure, are due to skeletal vibrations involving C–O stretching. From the IR spectrum of TMC in figure 5 (curve (b)), the decrease of the characteristic peaks of amino N–H vibration deformation at 1598 cm^{-1} and the obvious increase of $–CH_2$, $–CH_3$ vibrations at 2932, 2844 and 1489, 1380 cm^{-1} indicate successful substitution with methyl groups at C2–NH_2 in chitosan. The characteristic peaks of alcohol and a second alcohol located between 1160 and 1030 cm^{-1} did not change,

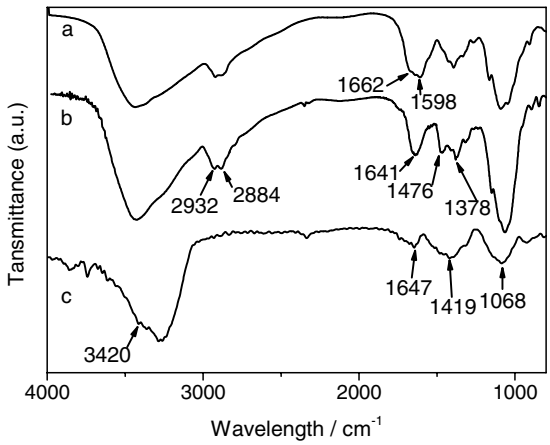

Figure 5. FTIR spectra of (a) chitosan, (b) TMC and (c) TMC-coated gold nanoparticles.

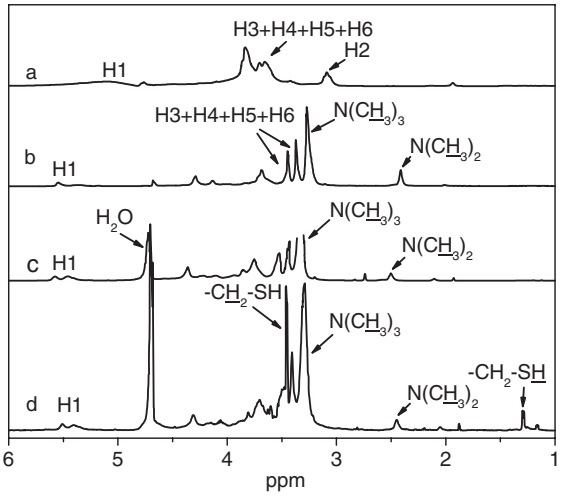

Figure 6. ^{1}H NMR spectra of (a) chitosan, (b) *N*-trimethyl chitosan chloride (TMC), (c) TMC-derivatized gold nanoparticles and (d) TMC-derivatized gold nanoparticles with the addition of mercaptoacetic acid.

confirming the lack of introduction of an alkyl group at C3–OH and C6–OH. However, by comparison with the FTIR spectrum of TMC, the disappearance of the $–CH_2$, $–CH_3$ vibrations at 2932, 2884 and 1476, 1378 cm^{-1} in the FTIR spectrum of the TMC-AuNP (figure 5, curve (c)) shows the partial loss of the C–H vibrations assigned to the methyl groups modified on the C2–NH_2 of chitosan. The decreasing and broadening absorption peaks in the range of 600–2000 cm^{-1} indicate the blockage by gold nanoparticles of the C–O and C–N vibrations in the chitosan skeletal structure. This indicates the existence of metallic nanoparticles resulting in an impediment to the polymer coating in IR vibrations. The most obvious changes in the IR absorption of $–CH_3$ shows that the methyl groups are possible functional groups close to the gold nanoparticles.

To reveal the functional groups interacting with the neighbouring gold nanoparticles (figure 1), ^{1}H NMR and ^{13}C NMR spectra were used for an intensive investigation. The ^{1}H NMR spectra of chitosan, TMC and TMC-coated gold nanoparticles are shown in figure 6. The ^{1}H NMR assignments of the chitosan (figure 6, curve (a)) are as follows: ^{1}H NMR (D_2O/F_3COOH) $\delta = 4.76$ (H1), $\delta = 3.09$ (H2), $\delta = 3.81$–3.43 (H3, H4, H5, H6), $\delta = 1.96$ ($NHCOC\underline{H}_3$) ppm [25, 26]. After modification, TMC can be easily dissolved in water at neutral pH. Compared with the ^{1}H NMR (D_2O) spectrum of chitosan, the ^{1}H NMR (D_2O) spectrum of TMC showed new peaks at $\delta = 3.25$ and 2.46 ppm which are assigned to the quaternary and tertiary amino groups, respectively (figure 6, curve (b)). Interestingly, the signal of H2 almost disappeared, and may be overlapped by the signal of the quaternary amino groups to form a strong peak. The signal of H1 was moved to the downfield by about $\delta = 5.54$ ppm due to the inductive effects of the substitute groups. The peak at $\delta = 3.24$ ppm showed increased intensity compared to the peak at $\delta = 2.40$ ppm, and the degree of substitution can be calculated from the integral in the spectrum (figure 6, curve (b)). The degree of substitution of the trimethylated (DQ%) and dimethylated groups (DT%) is determined by ^{1}H NMR [21] using the following equation (3):

$$\mathrm{DQ\%} = \left[\left(\int \mathrm{TM} \Big/ \int H\right) \times 1/9\right] \times 100,$$

$$\mathrm{DT\%} = \left[\left(\int \mathrm{DM} \Big/ \int H\right) \times 1/6\right] \times 100 \qquad (3)$$

where DQ% is the degree of quaternization as a percentage, $\int$ TM/ $\int$ DM is the integral of the trimethyl/dimethyl amino group (quaternary/tertiary amino) peaks at 3.24 and 2.40 ppm on the ^{1}H-NMR spectrum, and $\int H$ is the integral of the H1 peaks between 4.8 and 5.7 ppm on the ^{1}H-NMR spectrum. DQ% and DT% were calculated as 51.1% and 9.2%, respectively. These results confirmed that the main product is the quaternary derivative. Comparison with the ^{1}H NMR result of TMC shows that the ^{1}H NMR spectrum of the TMC-AuNPs (figure 6, curve (c)) is similar to that of the free TMC, except that the intensity of the fine structure of all the methyl protons of the latter for the modified $–N^+(CH_3)_3$ and $–N(CH_3)_2$ groups decreased. Broadening of the peaks assigned to the methyl groups is evident, which is attributed to the effect of the metallic centre on the ligands [27] and the 'solid like' nature of the chains [28].

The relatively low affinity of TMC towards gold nanoparticles in TMC-coated AuNPs was confirmed by using a ligand exchange reaction. We know that the interaction of S–Au bonds is much stronger than that of surface ion pairs. If the thiolate compound is added to a solution of TMC-AuNPs, a ligand exchange reaction occurs. In this experiment, mercaptoacetic acid ($HS–CH_2–COOH$) with the same molar ratio as the TMC units was added to the TMC-AuNP solution for ligand exchange. It was found that upon addition of mercaptoacetic acid, the colour of the TMC-AuNP solution immediately changed from orange to purple, which indicates the formation of S–Au bonds and the relatively low affinity of the surface ion pairs. Furthermore, ^{1}H NMR measurements were performed to prove the above speculation. Addition of mercaptoacetic acid leads to the release of functional groups, testified by the chemical shift and the integral of the methyl protons in the $–N^+(CH_3)_3$ before and after the addition of the mercaptoacetic acid. In the ^{1}H NMR spectrum of the TMC-AuNPs (figure 6, curve (c)), the chemical shift of the methyl

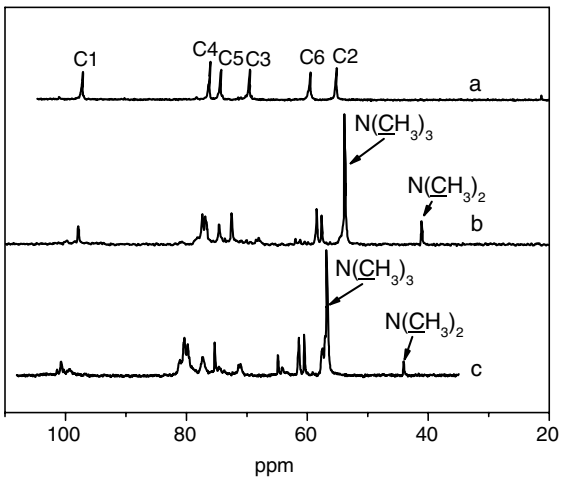

Figure 7. ^{13}C NMR spectra of (a) chitosan, (b) TMC and (c) TMC-coated gold nanoparticles.

protons in $-N^+(CH_3)_3$ groups is downfield ($\delta = 3.36$ ppm) due to the existence of gold nanoparticles as compared to the pure TMC ($\delta = 3.245$ ppm, figure 6, curve (b)). After addition of the mercaptoacetic acid, the chemical shift was back to $\delta = 3.28$ ppm (figure 6, curve (d)), confirming the release of the functional groups from the AuNPs. If we compare the integral of the $-N^+(C\underline{H}_3)_3$ peaks, the same conclusion can be drawn from the ^{1}H NMR results. The value of $\int \mathrm{TM}/\int H$ (the same meanings as in equation (3)) for pure TMC was 4.60. This value decreased to 4.34 for the TMC-AuNPs. After the addition of mercaptoacetic acid, this value increased to 5.31. This increase can be due to the release of $-N^+(C\underline{H}_3)_3$ groups. These phenomena are consistent with the conclusion drawn from the results of the FTIR spectra. The substituted methyl groups were the functional groups that locate beside gold nanoparticles, and resulted in the formation of AuNPs coated with the polymer shell structures.

Further evidence for the ligand mechanism proposed above was obtained from ^{13}C NMR spectroscopy. ^{13}C NMR assignments of chitosan (figure 7 curve (a)) are as follows: ^{13}C NMR (D_2O/F_3COOH)$\delta = 97.5$ (C1), $\delta = 76.5$ (C4), $\delta = 75$ (C5), $\delta = 70$ (C3), $\delta = 60$ (C6), $\delta = 55.6$ (C2) ppm [25, 26]. The ^{13}C NMR spectra for the substituted material, TMC, are presented in figure 7, curve (b). Compared with chitosan, the trimethylated and dimethylated signals respectively at $\delta = 53.8$ and 41.2 ppm are obvious. From the ^{13}C NMR spectrum, the intensity of the peak at 53.8 ppm for $-N(CH_3)_3^+$ groups is higher than the peak at $\delta = 41.2$ ppm for $-N(CH_3)_2$ groups, confirming the main product of TMC. The peak broadening and chemical shift of the methyl C in $-N^+(CH_3)_3$ groups is downfield ($\delta = 56.78$ ppm) in the ^{13}C NMR spectrum of TMC-AuNPs (figure 7, curve (c)) as compared to the pure TMC ($\delta = 53.8$ ppm, figure 7, curve (b)) and could be also due to the existence of gold nanoparticles.

Based on the results of FTIR, ^{1}H NMR and ^{13}C NMR spectra, we can conclude that the quaternary ammonium chloride groups play an important role in formation of TMC-coated gold nanoparticles. As shown in figure 1, $-N(CH_3)_3^+$ displays a tripod-like spatial conformation. The chloride ion (Cl^-) located between the $-N(CH_3)_3^+$ groups and gold nanoparticles formed a bridge to connect the metallic core and the polymer shell. In this structure, the chloride ions have electrostatic interactions with $-N(CH_3)_3^+$ and surface ion pairs on the gold nanoparticles. This special bridge structure, combined with the long chain framework of TMC, forms the polymer shell around the metallic nanoparticles. It is the repulsion effect between the charged polymers that prevent the possible aggregation of the metallic nanoparticle core, and bestows stability on the prepared nanoparticles in aqueous solution.

4. Conclusion

In this paper we introduce a simple method for preparing well-dispersed stable metallic nanoparticles with a narrow size distribution. This study shows that TMC is a very effective stabilizing agent for the preparation of gold nanoparticles. The ligand mechanism was investigated for the first time by FTIR, ^{1}H NMR and ^{13}C NMR spectra. The special bridge structure between the stabilizing agent and the metallic nanoparticles leads to a stable shell–core structure. In a neutral aqueous solution, TMC were coated around the metallic nanoparticles. The polymer shell with cations separated the metal cores from each other and prevented the aggregation of the polymer shell structure in aqueous environments. Successful preparation of TMC-stabilized silver and platinum nanoparticles proves the present method to be a general strategy for nanostructure formation. We are currently applying this approach to the synthesis of other metallic nanoparticles (e.g. Pd nanoparticles) and complexes such as Prussian Blue nanoparticles. It is anticipated that the TMC encapsulated gold nanoparticles will allow shell functionalization, biomolecule conjugation and the formation of AuNP-labelled biomolecules.

Acknowledgments

This work was supported by grants from the National Natural Science Foundation of China (NSFC, nos 20125515, 20375016, 20535010, 90206037) and the National Science Fund for Creative Research Groups (20521503).

References

[1] Daniel M C and Astruc D 2004 *Chem. Rev.* **104** 293
[2] Liz-Marzán L M 2004 *Mater. Today* **2** 26
[3] Brust M, Walker M, Bethell D, Schiffrin D J and Whyman R 1994 *J. Chem. Soc. Chem. Commun.* 801
[4] Mangeney C, Ferrage F, Aujard I, Marchi-Artzner V, Jullien L, Ouari O, Rékai E D and Laschewsky A 2002 *J. Am. Chem. Soc.* **124** 5811
[5] Ackerson C J, Jadzinsky P D and Kornberg R D 2005 *J. Am. Chem. Soc.* **127** 6550
[6] Woehrle G H, Brown L O and Hutchison J E 2005 *J. Am. Chem. Soc.* **127** 2172
[7] Lévy R, Thanh N T K, Christopher Doty R, Hussain I, Nichols R J, Schiffrin D J, Brust M and Ferring D G 2004 *J. Am. Chem. Soc.* **126** 10076
[8] Turkevitch J, Stevenson P C and Hillier 1951 *J. Discuss. Faraday Soc.* **11** 55
[9] Teranishi T, Kiyokawa I and Miyake M 1998 *Adv. Mater.* **10** 596
[10] Mayer A B R and Mark J E 1998 *Eur. Polym. J.* **34** 103
[11] Bunge S D, Boyle T J and Headley T J 2003 *Nano Lett.* **3** 901
[12] Huang H and Yang X 2004 *Biomacromolecules* **5** 2340

[13] Dos Santos D S, Goulet P J G, Pieczonka N P W, Oliveira O N and Aroca R F 2004 *Langmuir* **20** 10273
[14] Miyama T and Yonezawa Y 2004 *Langmuir* **20** 5918
[15] Karadas F, Ertas G, Ozkaraoglu E and Suzer S 2005 *Langmuir* **21** 437
[16] Fink J, Kiely C J, Bethell D and Schiffrin D J 1998 *Chem. Mater.* **10** 922
[17] Murata J I, Ohya Y and Ouchi T 1996 *Carbohydr. Polym.* **29** 69
[18] Kotzé A F, Lueben H L, de Leeuw B J, de Boer B G, Verhoef J C and Junginger H E 1997 *Pharm. Res.* **14** 1197
[19] Thanou M, Verhoef J C, Verheijden J H M and Hunginger H E 2001 *Pharm. Res.* **18** 823
[20] Hamman J H, Stander M and Kotzé A F 2002 *Int. J. Pharm.* **232** 235
[21] Thanou M, Verhoef J C, Marbach P and Junginger H E 2000 *J. Pharm. Sci.* **89** 951
[22] Van der Merwe S M, Verhoef J C, Kotzé A F and Junginger H E 2004 *Eur. J. Pharm. Biopharm.* **57** 85
[23] Sieval A B, Thanou M, Kotzé A F, Verhoef J C, Brussee J and Junginger H E 1998 *Carbohydr. Polym.* **36** 157
[24] Youk J H, Park M K, Locklin J, Advincula R, Yang J and Mays J 2002 *Langmuir* **18** 2455
[25] Hirai A, Odani H and Nakajima A 1991 *Polym. Bull.* **26** 87
[26] Le Dung P, Milas M, Rinaudo M and Desbriers J 1994 *Carbohydr. Polym.* **24** 209
[27] Terrill R H *et al* 1995 *J. Am. Chem. Soc.* **117** 12537
[28] Badia A, Singh S, Demers L, Cuccia L, Brown G R and Lennox R B 1996 *Chem. Eur. J.* **2** 359